IEEE Access
Multidisciplinary ⋮ Rapid Review ⋮ Open Access Journal

Received February 4, 2022, accepted February 28, 2022, date of publication March 17, 2022, date of current version April 7, 2022.

Digital Object Identifier 10.1109/ACCESS.2022.3160473

SIGW Based MIMO Antenna for Satellite Down-Link Applications

M. S. H. SALAH EL-DIN[1,2], SHOUKRY I. SHAMS[3], (Member, IEEE), A. M. M. A. ALLAM[4], ABDELHAMID GAAFAR[1], HADIA M. ELHENNAWY[2], (Member, IEEE), AND MOHAMED FATHY ABO SREE[1]

[1]Department of Electronics and Communications Engineering, Arab Academy for Science, Technology and Maritime Transport, Cairo 451913, Egypt
[2]Department of Electronics and Communications Engineering, Ain Shams University, Cairo 11517, Egypt
[3]Department of Electrical and Computer Engineering, Concordia University, Montreal, QC H3G 1M8, Canada
[4]Head of Information Technology, GUC, Cairo 101516, Egypt

Corresponding author: Mohamed Fathy Abo Sree (mohamed.fathy@aast.edu)

ABSTRACT In this paper, a 4-port multi-input multi-output (MIMO) antenna based on substrate integrated gap wave guide (SIGW) is presented for down-link satellite applications. The proposed MIMO antenna consists of four rectangular-shaped radiating slots, which are fed via SIGW to minimize dispersion and insertion loss. Firstly, single antenna element (reference antenna) is designed to have impedance matching and stable radiation pattern over the bandwidth 13.4-13.65 GHz. Afterward, different antenna configurations are studied to combine four identical elements of the reference one for the sake of minimizing mutual coupling between them. In this work, the edge-to-edge separation between the antenna elements for orthogonal and opposite orientations are 9.3mm and 17.3mm, respectively. The mutual coupling between antenna elements is suppressed by etching the upper ground in the region between the antenna elements. Moreover, further optimization is carried out by changing the dimensions of the etched slot to reach higher isolation between radiating slots for better MIMO diversity performance. With this approach, the realized gain is increased by 3-dBi and the maximum mutual coupling achieved at 13.5 GHz between port (1,2) and port (1,3) are -63 dB and -78 dB, respectively with isolation enhancement of 38 dB between port (1,2) and 48 dB between port (1,3). Both simulated and measured results indicate that the proposed antenna has a bandwidth of 13.3-13.8 GHz, with a high isolation greater than 40 dB. Furthermore, the realized antenna gain is around 9-dBi with radiation efficiency of 86%. In addition, the designed MIMO antenna offers excellent radiation characteristics and stable gain over the whole operating band. To explore the diversity of the MIMO system the envelope correlation coefficient (ECC), multiplexing efficiency (ME), diversity gain (DG), channel capacity loss (CCL) and total active reflection coefficient (TARC) are studied. Finally, good consistency between simulation and measured outcomes is obtained confirming the validity of the MIMO antenna for real life satellite application systems.

INDEX TERMS MIMO antenna, SIGW, satellite downlink applications.

I. INTRODUCTION

With the rapid evolution in the modern wireless communication systems, the great demand for high data rate, high channel capacity and reliability is dramatically increasing for satellite technology, earth monitoring, mobile communication and radar. Single-band antennas with different adaptable polarizations has attracted attention for such applications as it can improve the data resolution, transmission rate and dramatically reduce signal interference [1]. To maximize channel efficiency and increase data integrity, the multiple input multiple output (MIMO) system has been one of the most suitable and promising technology as it is well suited for high capacity, high data rate and high reliability requirements [2]. In addition, MIMO antenna system can alleviate the effect of multipath, conduct diversity gain and multiplexing efficiency [3].

The salient features of the MIMO based systems in wireless communication generated the interest for satellite communication (SATCOM) systems to profit from such significant achievements [4]. The satellite channel for fixed satellite applications in frequency band above 10 GHz is

The associate editor coordinating the review of this manuscript and approving it for publication was Shah Nawaz Burokur.

dominated by a strong line of sight (LOS) path which may lead to lack in the spatial MIMO channel matrix. Subsequently, the MIMO may not appear as a candidate for SATCOM to provide spatial diversity. However, SATCOM can benefit from MIMO using orthogonal polarizations, multiple satellites, multiple ground terminals and multiple user concepts even in absence of scattering in SATCOM propagation path. In addition, high MIMO gains in strong LOS channels can be achieved with particular antenna geometries scenarios [5], [6].

Satellite applications in Ku-band such as telecommunication broadcasting, direct-to-home services, tracking data relay and global position system (GPS) can benefit from the outstanding features of MIMO antenna systems [7], [8]. To enhance the performance of MIMO based system, low correlation between antenna elements is needed. This can be achieved by increasing the isolation between the antenna ports. Lower isolation may lead to degradation in the radiation pattern of each element of the multi-element system. As a result, it may lower antenna efficiencies and increase correlation coefficients [9]. Thus, the primary aim of MIMO antenna design is to reduce correlation between the received signals.

Various techniques have been used to increase isolation between MIMO antenna elements including neutralization technique [10], orthogonal feeding or elements, which results in considerable polarization and pattern diversity [11], [12], simultaneous matching [13] and etching slits in the middle of the ground-plane [14]. In addition, electromagnetic band gap (EBG) substrates, defected ground structure (DGS), metamaterials, metasurfaces, split ring resonator and parasitic resonators have been presented to reduce coupling between antenna elements [15]–[20]. These techniques require considerable circuit board space. In another approach the isolating slot is etched between the antenna elements [21]. Various slot configurations have been explored including a vertical slot [22], a T-shaped slot [23], F-shaped stubs [24] and L-shaped slot [25]. Although these isolating slots minimize the mutual coupling between the radiating antennas, they do not improve the system gain.

Numerous antenna design methods have been proposed in the Ku–band to reduce mutual coupling between MIMO antenna elements as well as gain enhancement and reduction in the overall size of the antenna [26]–[32]. In [26], meta-surface isolator was used as a decoupling structure for 2-element patch MIMO antenna to offer an average of 10 dB of mutual coupling suppression with average gain enhancement of 2 dBi in the Ku-band. Also, linear slots were placed between radiating oval shaped slots of 4-element MIMO antenna to reduce mutual coupling of about 20 dB in Ku-band with gain improvement of 2 dB in [27]. Moreover, two port textile MIMO antenna with two half ring shaped antenna elements was presented in [28]. The ground plane is defected to achieve a minimum isolation of 15.5 dB in the Ku-band. In [29], a four-element compact wideband MIMO antenna with four T-shaped radiating elements was introduced. The minimum isolation of 15 dB and maximum gain of 5 dBi were achieved by using reduced ground plane and stubs at the bottom ground. Also, in [30], inverted pair of L-shaped stubs placed in the ground of dual patched wideband MIMO antenna are used to obtain better isolation of about 20 dB with peak gain of 5.32 dBi. The main disadvantage of such system is the complexity of design and low realized gain. Moreover, some of the MIMO systems available in the literature have good miniaturization with good isolation characteristics but they have a drawback in terms of poor gain. Thus, this makes them less suitable for wireless applications. To improve system gain, a dumbbell shaped slot is located between two inverted E-shaped monopole elements to decrease mutual coupling in [31]. A high isolation of more than 20 dB is presented with average gain of 8 dBi in the Ku-band. Also, in [32], a 4×6 array MIMO antenna is used to achieve high antenna gain but the design was bulky. Although a significant effort in the recent years has been directed to introduce featured MIMO antennas with reliable diversity parameters, there is a still a room of improvement to achieve higher isolation along with a high stable gain along the operating band which remains a challenging task.

In this paper, a four-port MIMO antenna system is designed, fabricated and measured for satellite down link application covering frequency from 13.4-13.65 GHz. It exhibits an isolation over 40 dB with gain around 9 dBi. The design is based on orthogonal orientation of the antenna elements in conjunction with slots etched in the ground plane between the antenna elements. A configuration without any isolation technique is used as a reference of evaluation for the isolation and gain enhancement. The feeding network is substrate integrated gap waveguide (SIGW) based technology. It is used to inhibit the dispersion relative to either microstrip or coplanar traditional feeding networks. The antenna is considered a compact one taking into consideration the topology of MIMO system based on GW technology.

II. FEEDING NETWORK DESIGN AND TRANSITION

In this section, the design of proposed feeding network is presented. It is SIGW of mushroom unit cell which is based on GW technology. The main feature of the GW technology is guiding the signal over ridge surrounded by high impedance textured surface called Artificial Magnetic Conductor (AMC). It creates a stop band forcing all parallel-plate modes to be prohibited [33]. Three rows of AMC structure can be enough to inhibit the leakage and prevent radiation [34]. One of the key elements in the GW configuration is the design of the unit cell that constructs the AMC surface.

As shown in Fig. 1, the unit cell consists of four layers; bottom and top ground layers which are made of lossy copper annealed and two substrate layers which are sandwiched between them. The substrate material for the lower layer is Rogers RO4350B with relative dielectric constant of 3.66 and for the upper layer is Rogers RO4003C of 3.55. The array of periodic metallic vias implanted on the bottom layer and ended with a layer of periodic patches representing

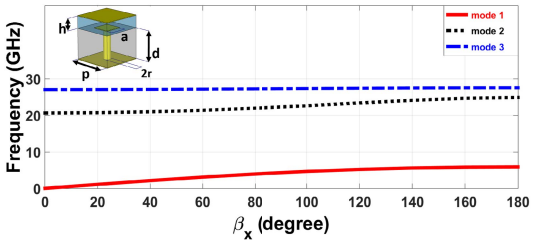

FIGURE 1. Dispersion diagram of the unit cell.

the mushroom structure. This unit cell is placed periodically around the ridge forming SIGW transmission line. The dispersion diagram of the mushroom unit cell and the transmission line are carried out using Eigen mode solver (CST microwave studio) and are illustrated in Fig. 1 and Fig. 2, respectively. As it can be seen from Fig. 2, there is a band-gap between 6 GHz to 20 GHz. In this band-gap, the fields will be confined over the ridge with a quasi-TEM field distribution resulting in a dominant mode with minimal dispersion [35]. The dimensions of the unit cell and ridge are demonstrated in table 1.

TABLE 1. Dimensions of the unit cell and ridge.

Parameter	Description	Value(mm)
d	Substrate thickness (lower layer)	1.524
a	Patch width	2.5
r	Radius of via	0.5
h	Substrate thickness (upper layer)	0.203
wr	Ridge line width	2.4
p	Unit cell width	3.5
wm	Width of quarter wavelength transformer	1.2
ws	Width of the microstrip line	0.45

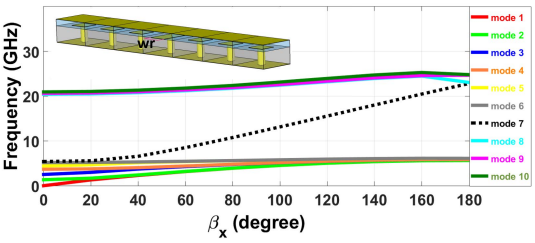

FIGURE 2. Dispersion diagram of the ridge gap transmission line.

Transition between SIGW and microstrip is required to excite and measure GW structure. For the sake of feeding the proposed antenna, a microstrip to SIGW transition is designed to operate in the Ku-band. It is a microstrip line structure with characteristics impedance 50 ohm as shown in Fig. 3(a). It is implemented on ROGERS RO4003C with relative dielectric constant 3.55, thickness 0.203mm and loss tangent 0.0027. The width of the microstrip line (ws) is 0.45mm. To connect the transition with ridge, the transition is turned upside down such that the microstrip line touches the upper surface of the ridge. Quarter wavelength transformer with optimization is used to match the transition with feeding

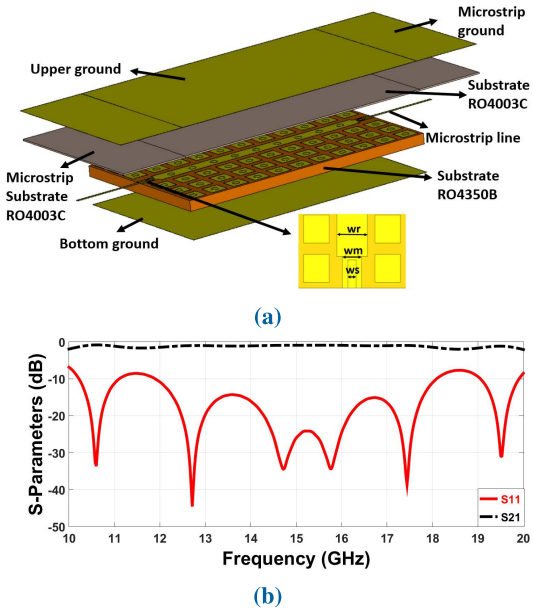

FIGURE 3. Microstrip-SIGW transition (a) 3D structure (b) Simulated s-parameters.

network. The s-parameter of the microstrip-SIGW transition is illustrated in Fig. 3(b). The reflection coefficient shows a behavior better than -10 dB over the desired Ku-band. Also, it is clear that the transmission coefficient is close to -1 dB, which is due to the insertion losses from the microstrip transitions input/output lines in the whole operational bandwidth.

III. MIMO ANTENNA DESIGN

A. SINGLE-ELEMENT STRUCTURE

The design of MIMO antenna systems usually starts with a single element. The geometrical configuration of the proposed single element antenna structure is illustrated in Fig. 4. It is designed to operate in 13.4-13.65 GHz frequency range for downlink satellite applications. It consists of SIGW structure to feed rectangular shaped slot antenna which is etched in the top ground plane to drive the electromagnetic waves toward the z-direction. The slot antenna has the dimensions of 5.85 mm x 7.37 mm to resonate at 13.5 GHz based on microstrip patch antenna design equations [36]. Two quarter

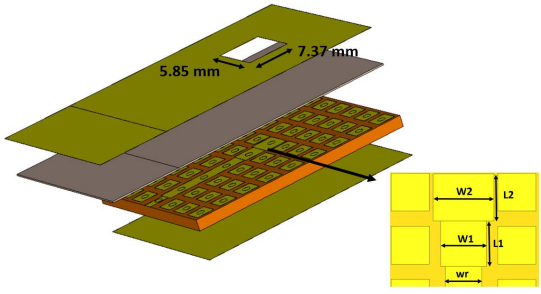

FIGURE 4. Proposed 3D configuration for the single element MIMO antenna with matching section between ridge and slot antenna.

TABLE 2. Dimensions of the matching section.

Parameter	Value(mm)
W1	3
W2	4
L1	3
L2	3.1

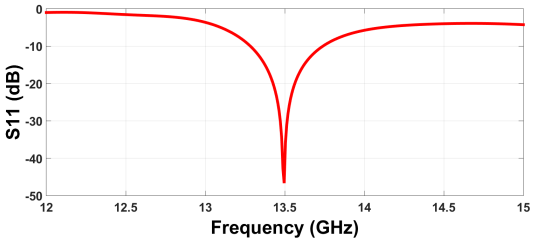

FIGURE 5. Simulated reflection coefficient of single element MIMO antenna.

wavelength transformer sections are used to provide matching between the guiding structure and the antenna radiating slot. An optimization process is performed to obtain a better matching level with reflection coefficient depicted in Fig. 5. It is clear that the operating band conducts the satellite application requirements (13.4-13.65 GHz). The dimensions of matching stages are demonstrated in table 2.

$$Width = \frac{c}{2f_r}\sqrt{\frac{2}{\epsilon_r + 1}} \tag{1}$$

$$\epsilon_{reff} = \frac{\epsilon_r + 1}{2} + \frac{\epsilon_r - 1}{2}[1 + 12\frac{h}{W}]^{-1/2} \tag{2}$$

$$L = L_{eff} - 2\Delta L \tag{3}$$

where

$$L_{eff} = \frac{c}{2f_r\sqrt{\epsilon_{reff}}} \tag{4}$$

$$\Delta L = 0.412h\frac{[\epsilon_{reff} + 0.3]}{[\epsilon_{reff} - 0.258]}\frac{[\frac{w}{h} + 0.264]}{[\frac{w}{h} + 0.8]} \tag{5}$$

B. TWO-ELEMENT MIMO STRUCTURE

The two-element structure of the proposed MIMO antenna is discussed in this section. First, the orientation of antenna elements is studied. Fig. 6 illustrates the two configurations which are used in the antenna design. In the first configuration shown in Fig. 6(a), the two elements have 90° between them (orthogonal orientation) with spacing of 9.3 mm between the edges of two antennas. While elements in the second configuration are placed in opposite orientation (180°) with spacing of 17.3 mm between the edges, as illustrated in Fig. 6(b). The simulated scattering parameters of the two antenna configurations are demonstrated in Fig. 7. It is apparently obvious that the antenna with opposite orientation exhibits lower mutual coupling of -29 dB between elements due to the spacing. On the other hand, antenna with orthogonal orientation has mutual coupling lower than -25 dB within the entire

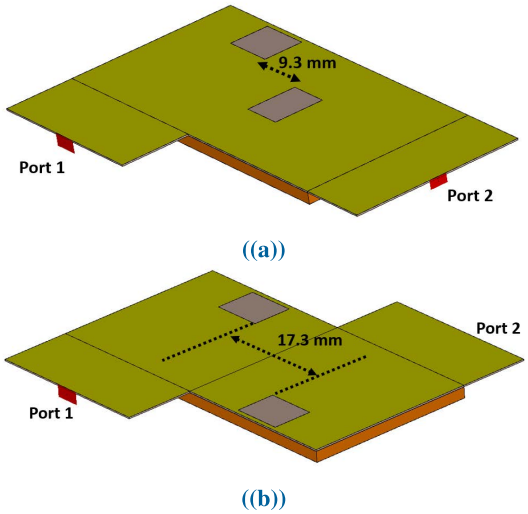

FIGURE 6. Proposed 3D configuration for the two element MIMO antenna. (a) Orthogonal orientation. (b) Opposite orientation.

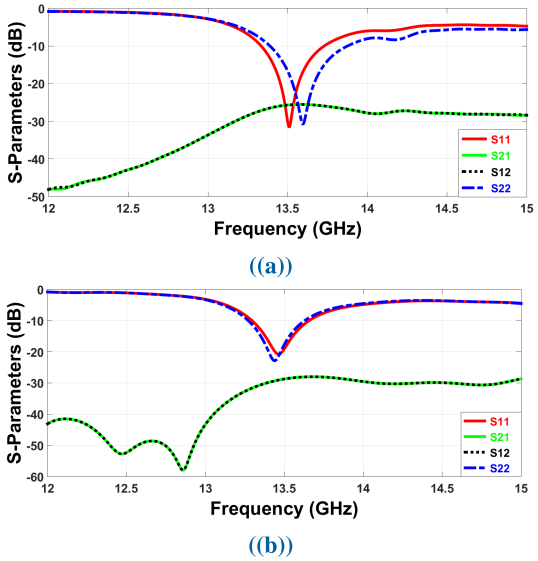

FIGURE 7. Simulated s-parameters of two element MIMO antenna. (a) Orthogonal orientation. (b) Opposite orientation.

frequency band. Finally, it can be concluded that the two orientations (90° and 180°) have acceptable low mutual coupling which will lead to good MIMO antenna performance.

C. FOUR-ELEMENT MIMO STRUCTURE

1) ANTENNA WITHOUT ISOLATION ENHANCEMENT TECHNIQUE

Based on the aforementioned discussion, the four-element MIMO antenna is arranged as depicted in Fig. 8(a). The two orientations of previous section are combined to form four-element MIMO system. The antenna element at port 1 is oriented orthogonally on antennas at port 2 & 4 and in opposite direction with the antenna at port 3. The proposed four-element MIMO antenna is fabricated as shown

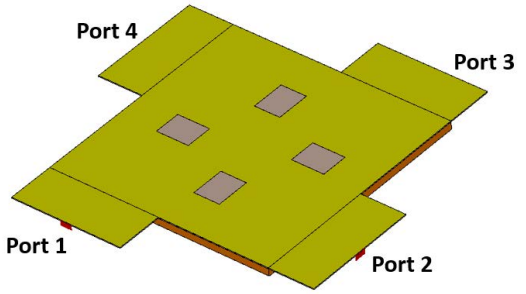

((a))

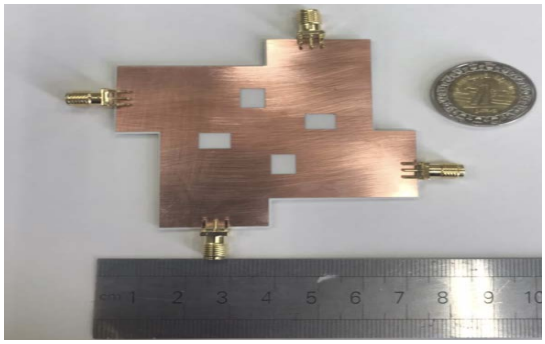

((b))

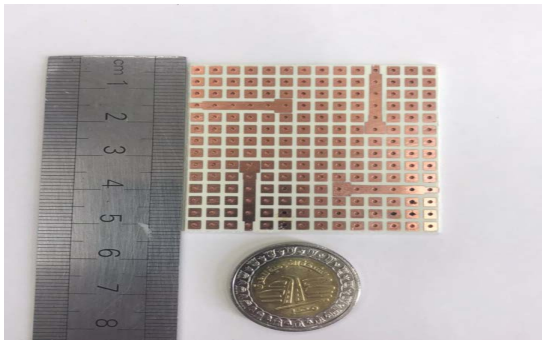

((c))

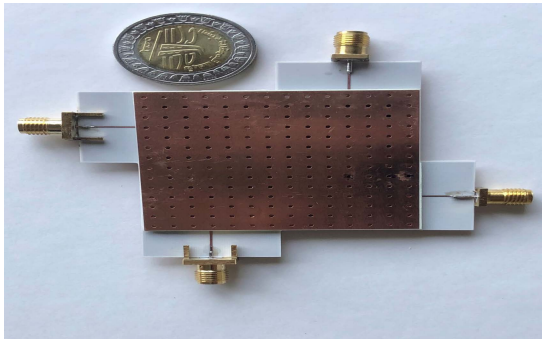

((d))

FIGURE 8. Proposed 3D model for the four element MIMO antenna. (a) Simulated model. (b) Top view of fabricated model. (c) Top view of fabricated model without top layer. (d) Back view of fabricated model.

in Fig. 8. Fig. 9 illustrates the simulated and the measured scattering parameters of the proposed antenna which shows good trend between both results. In Fig. 9(a), it is obvious that the antenna operates at frequency band from 13.28 GHz

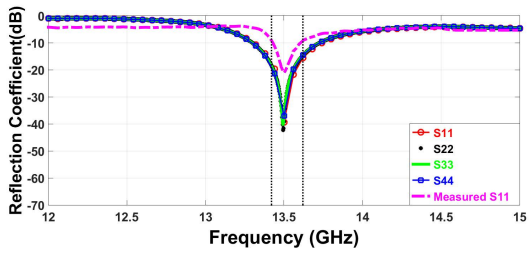

((a))

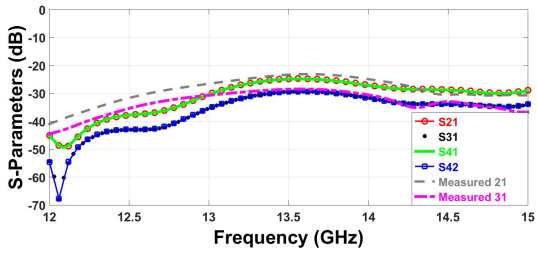

((b))

FIGURE 9. Simulated and measured s-parameters of four element MIMO antenna. (a) Reflection coefficients. (b) Coupling coefficients.

to 13.73 GHz with good reflection coefficients performance lower than -10 dB at all ports which meets the intended satellite application. Furthermore, Fig. 9(b) presents the measured and simulated coupling coefficients (S21, S31, S41, S32, and S42). The results have mutual coupling of -25 dB between ports (1,2), ports (1,4), and ports (2,3) while ports (2,4) and ports (1,3) have mutual coupling of -30 dB. From these results, it is clear that S21, S41 and S32 are identical. Same for S31 and S42 which are perfectly matched. Thus, S21 and S31 results are fair enough for studying the effect of s-parameters of the proposed MIMO antenna system.

2) ANTENNA WITH ISOLATION ENHANCEMENT TECHNIQUE

To get higher isolation between antenna elements, the upper ground plane of the presented antenna is subjected to different modifications. First, the conductor of the upper ground is etched in the middle position between the antenna elements (Antenna A) to suppress the surface currents, as shown in Fig. 10. An optimization process on width 'Wc' is conducted to achieve more isolation with selected values of 'Wc', as demonstrated in Fig. 11. It is clear that 'Wc' of 0.8 mm reduces the mutual coupling (S21) and (S31) by 2 dB and 5 dB compared to antenna with no enhancement technique, respectively. Further modification is accomplished on the etched slots (Antenna B), as shown in Fig. 12. Fig. 13 shows a parametric sweep on length 'Lc' to achieve higher isolation. It is obvious that 'Lc' of 20.7 mm enhances the isolation between port (1,2) and (1,3) by 5 dB and 20 dB, respectively. It is clear that the orthogonal orientation has dominant effect on the isolation. To achieve higher isolation enhancement and gain especially between port (1,2), the slot is segmented into three cascaded linear slots with spacing 'S', as depicted in Fig. 14 (Antenna C). As shown in Fig. 15,

TABLE 3. S-parameters and gain comparison between MIMO antenna with and without proposed isolation technique.

Parameter	Antenna with no slots	Antenna A	Antenna B	Antenna C
Max suppression on S21(dB)	25	27	30	63
Max suppression on S31(dB)	30	35	45	78
Gain (dBi)	5.5	7.3	7.3	8.8

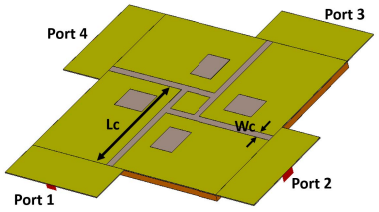

FIGURE 10. 3D configuration of antenna A.

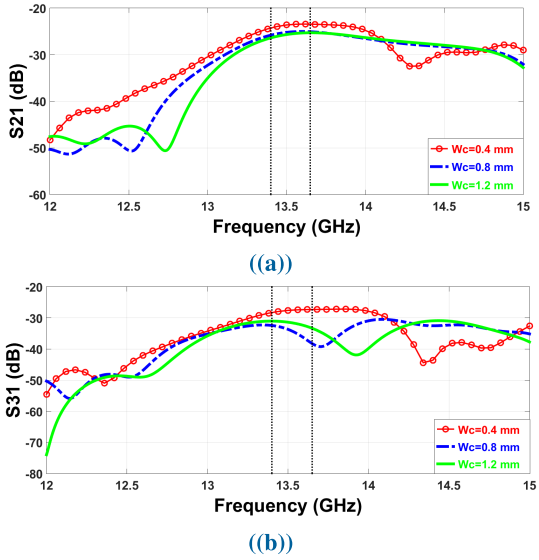

FIGURE 11. Simulated s-parameters of antenna A with the variation of Wc. (a) S21. (b) S31.

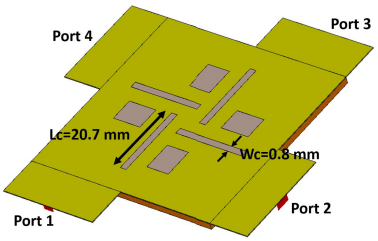

FIGURE 12. 3D configuration of antenna B.

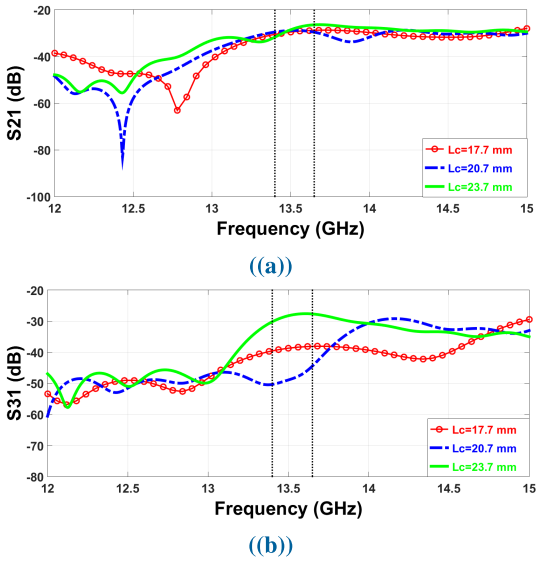

FIGURE 13. Simulated s-parameters of antenna B with the variation of Lc. (a) S21. (b) S31.

further optimization is held on the lengths of slots 'Xc' and 'Yc' to achieve better isolation. It is clearly obvious that antenna with 'Xc' of length 12.5 mm and 'Yc' of length 3.9 mm shows the best isolation enhancement. The isolation between port (1,2) is better that 40 dB in the whole bandwidth, while the magnitude of S31 is lower than -45 dB. Perhaps this enhancement is due to the suppression of higher order modes conducted from segmented slots. The simulated and measured reflection coefficient of the optimized design is depicted in Fig. 15(c), which shows good agreement. On the other hand, one can notice that the reflection coefficient is nearly the same before and after the enhancement process. Current density distribution over the proposed MIMO antenna with and without isolation enhancement technique are illustrated in Fig. 16. It is observed that surface current is suppressed at the adjacent radiating antennas by introducing the three cascaded linear slots. Thus, this decoupling technique plays a vital role for preventing the current flow to the other antenna which leads to higher isolation. Regarding the antenna gain, Fig. 17 shows that the proposed decoupling technique increases the average realized gain by 3 dBi to reach a gain of 8.8 dBi. Due to effective impedance matching, radiation efficiency reaches around 86% as seen in Fig. 18. Table 3 shows a comparison between s-parameters and gain of MIMO antenna with and without the proposed isolation technique. The radiation properties of the MIMO antenna with and without the proposed isolation technique are plotted in Fig. 19. It is clear that no significant degradation in the radiation pattern has been observed.

IV. DIVERSITY PERFORMANCE OF THE DESIGNED MIMO ANTENNA

A. THEORETICAL BACKGROUND

Several important parameters are analyzed to evaluate the diversity performance of the proposed MIMO antenna. The parameters used to serve this purpose are the envelope correlation coefficient (ECC), diversity gain (DG), channel capacity loss (CCL), multiplexing efficiency (ME) and total active reflection coefficient (TARC).

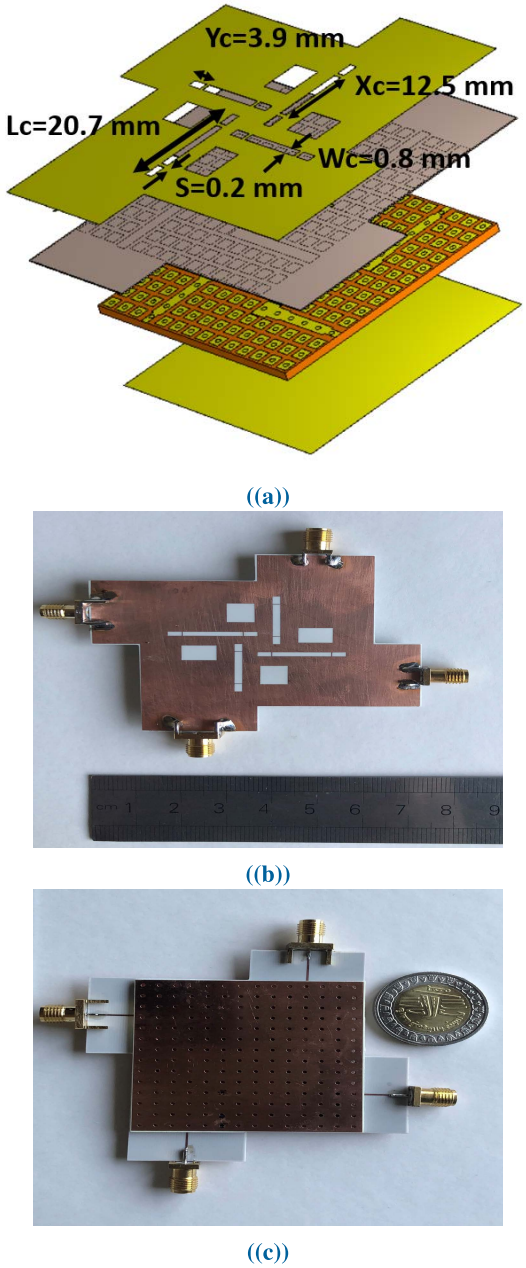

FIGURE 14. Proposed 3D model for antenna C. (a) Simulated model. (b) Top view of fabricated model. (c) Back view of fabricated model.

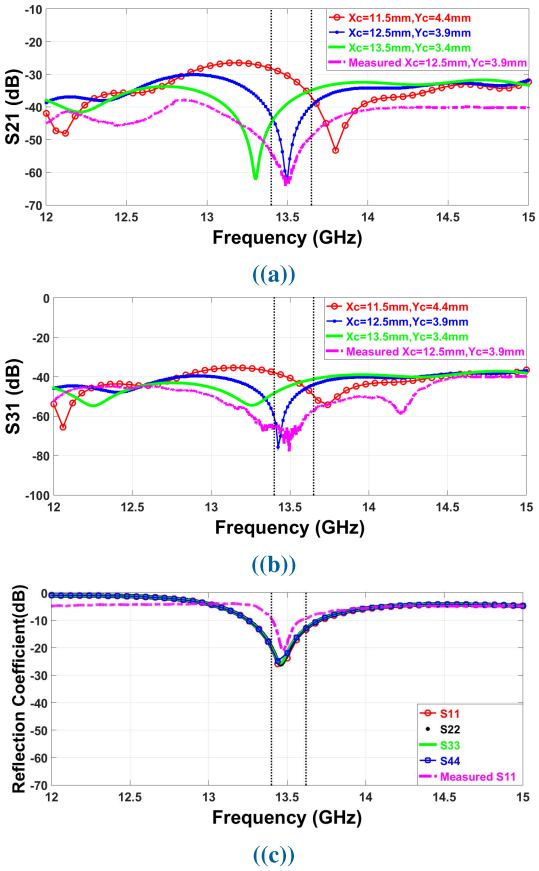

FIGURE 15. Simulated and measured s-parameters of proposed MIMO antenna C with the variation of Xc and Yc. (a) S21. (b) S31. (c) Reflection coefficient.

The first parameter is the ECC which measures the degree of correlation between different antenna elements of MIMO structure [37]. Lower ECC means lower the degree of dependence between the antenna elements. Thus, higher MIMO diversity performance. The ECC can be calculated from both the far field radiation pattern and scattering parameters as in equations (6) and (7), respectively [29], [37].

$$\rho_{eij} = \frac{|\int\int 4\pi[F_i(\theta,\phi)] \bullet [F_j(\theta,\phi)d\Omega]|^2}{\int\int 4\pi|F_i(\theta,\phi)|^2 d\Omega \int\int 4\pi|F_j(\theta,\phi)|^2 d\Omega} \quad (6)$$

where i,j = 1, 2, 3, 4, ρ_{eij} is the ECC between ith and jth antenna elements, while F_i (θ, ϕ) is the 3D radiation pattern field with excitation at port "i" and "•" denotes the hermitian product and "Ω" is the solid angle.

$$\rho_{eij} = \frac{|S_{ii}^* S_{ij} + S_{ji}^* S_{jj}|^2}{(1-|S_{ii}|^2-|S_{ji}|^2)(1-|S_{jj}|^2-|S_{ij}|^2)} \quad (7)$$

where "*" is the complex conjugate of the s-parameter. However, it is important to mention that computing the ECC values from s-parameters is not accurate and underestimates its values when evaluating any lossy antenna. Subsequently, the values obtained from far-field radiation patterns are more practical as they have higher accuracy [38]. On the other hand, this process requires complex and advanced calculations. For good MIMO antenna diversity, ECC should be lower than the acceptable limit 0.5 [2].

Diversity gain (DG) is another important parameter, obtained from ECC, to evaluate the performance of the MIMO antenna system, defined as [2]:

$$DG = 10\sqrt{1-(ECC)^2} \quad (8)$$

It is observed that the relationship between the correlation and diversity gain are inversely proportional, as seen in equation (8). Thus, a larger DG value indicates a better MIMO

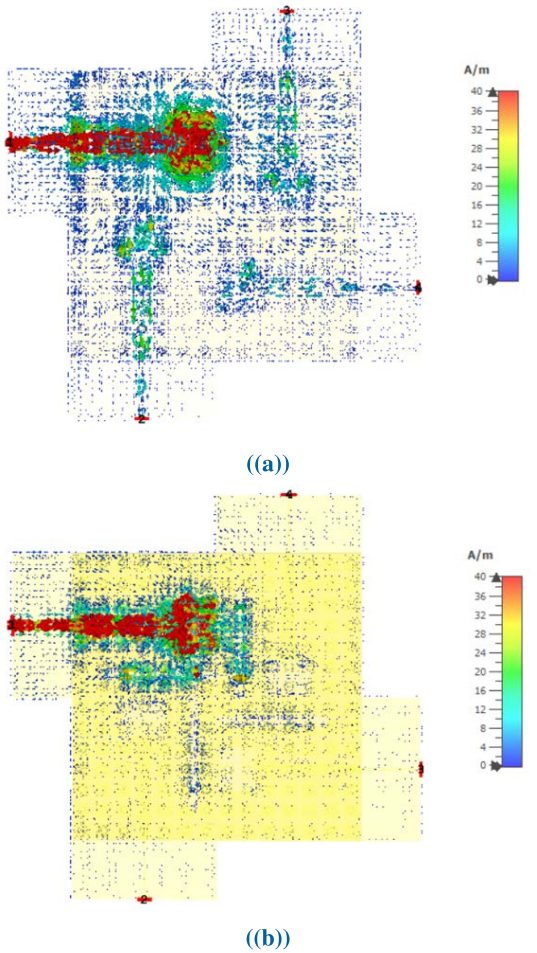

FIGURE 16. Surface current distribution over proposed MIMO antenna at 13.5 GHz (a) Without isolation enhancement technique. (b) With isolation enhancement technique.

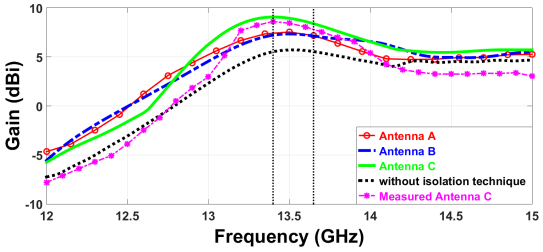

FIGURE 17. Realized gain comparison between different antenna configurations.

antenna performance. Since the DG is related to ECC, it can be calculated from both the far field radiation pattern and scattering parameters. The third one is CCL which defines the maximum reachable limit of the information transmission rate [39]. In other words, it measures the optimum information transmission rate [39]. Smaller CCL means the easier signal to transmit with lower losses. To have good diversity performance for MIMO antenna, CCL value should to be smaller than the acceptable value 0.4 bps/Hz [38].

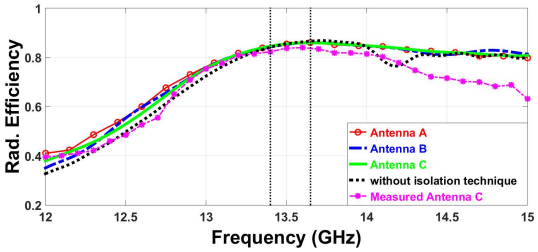

FIGURE 18. Radiation efficiency comparison between different antenna configurations.

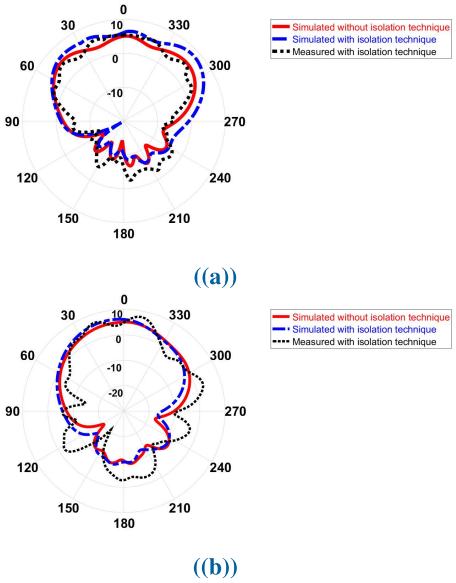

FIGURE 19. Simulated radiation pattern performance of the proposed MIMO antenna C with and without the isolation enhancement technique at 13.5 GHz. (a) $\phi = 0°$. (b) $\phi = 90°$.

For a four-port MIMO antenna system, it is mathematically expressed in equation (9) [39].

$$C_{loss} = -log_2 det(X^R) \tag{9}$$

where

$$X^R = \begin{bmatrix} X_{11} & X_{12} & X_{13} & X_{14} \\ X_{21} & X_{22} & X_{23} & X_{24} \\ X_{31} & X_{32} & X_{33} & X_{34} \\ X_{41} & X_{42} & X_{43} & X_{44} \end{bmatrix} \tag{10}$$

$$X_{ii} = 1 - \sum_{n=1}^{4} |S_{ij}|^2 \tag{11}$$

$$X_{ij} = -(S_{ii}^* S_{ij} + S_{ji}^* S_{ij}) \tag{12}$$

To have more evaluation on the MIMO antenna system, the ME has been computed. It is defined as the power of the real antenna over the power of the ideal one. It is the power ratio between the real antenna and the ideal one [37]. The maximum multiplexing efficiency has been calculated as [38]:

$$\eta_{max} = \sqrt{\eta_i \eta_j (1 - |\rho_{eij}|^2)} \tag{13}$$

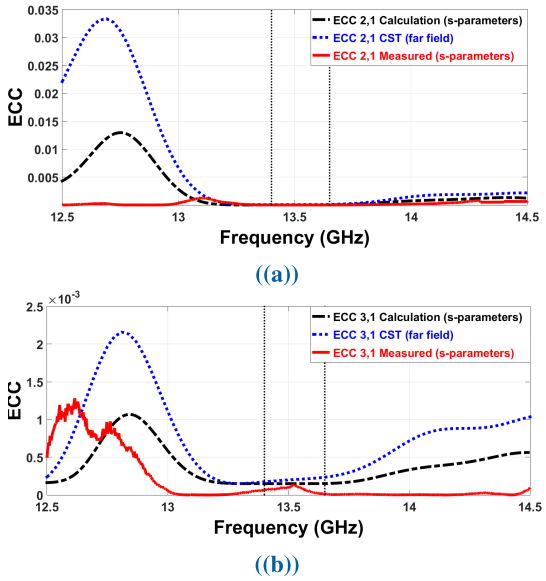

FIGURE 20. The ECC performance of the proposed four-element MIMO antenna. (a) between port 1 and 2. (b) between port 1 and 3.

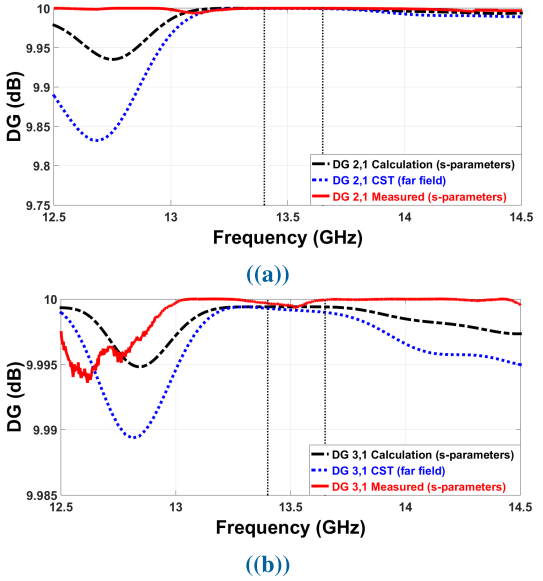

FIGURE 21. The DG performance of the proposed four-element MIMO antenna. (a) between port 1 and 2. (b) between port 1 and 3.

where η_i is the total efficiency of the i^{th} antenna elements and ρ_{eij} is the magnitude of complex correlation coefficients between ith and jth antenna elements.

The last parameter is TARC which is defined as the square root of the total reflected power divided by the square root of the total incident power [3], [29]. It represents the effective operating bandwidth of MIMO antenna system as it can be calculated from the S-parameters [12]. It is considered an important parameter because it accounts the inter-port coupling, port matching, and the effect of the random phases of incoming signals into each antenna element, therefore describing the performance in a more realistic situation. Under certain conditions, the random phases of incoming signals have an important impact on MIMO array behavior, and TARC is the only MIMO parameter that considers this information. For four-port MIMO antenna, the TARC expression can be calculated as the following equation [39]:

$$TARC = \frac{\sqrt{\sum_{i=1}^{4}|S_{i1} + \sum_{n=2}^{4} S_{in}e^{j\theta_{n-1}}|^2}}{2} \qquad (14)$$

where Θ is the excitation phase difference between the two ports. For a MIMO communication system, the TARC value should be <0 dB [3].

B. SIMULATED AND MEASURED RESULTS

Fig. 20 illustrates the ECC metric. It depicts the simulated ECC based on far field equation (6) using (FDTD) (CST Microwave studio), the calculated and the measured ECC based on equation (7). The value of the ECC between port (1,2) at the frequency band is below 10×10^{-5}, 0.25×10^{-5} and 10.6×10^{-5} extracted from simulated, the measured, and calculated results, respectively. While the ECC between port (1,3) at the operating band is below 8.7×10^{-5}, 0.12×10^{-5} and 0.17×10^{-6}, respectively. It is observed that calculated and measured values are well matched. Moreover, the corresponding DG values are illustrated in Fig. 21. It is obvious that the obtained DG is around 10 dB within the operating bandwidth. The calculated and measured CCL are shown in Fig. 22. It shows that the CCL value at the entire operating band is below 0.4 bps/Hz. The simulated, measured and calculated ME are around -1 dB within the band from 13.4 GHz to 13.65 GHz, as illustrated in Fig. 23. Finally, Fig. 24 clearly shows that the value of TARC for the proposed antenna is < -10 dB for the entire operating band.

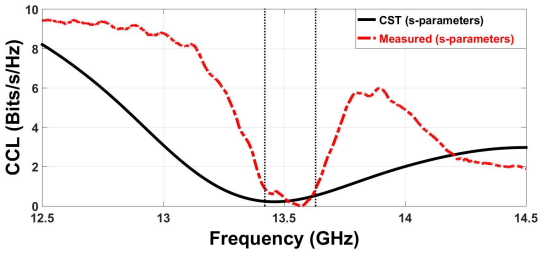

FIGURE 22. The CCL performance of the proposed four-element MIMO antenna.

Nevertheless, the measured results may show a little deviations with the simulated ones and this can be due to the fabrication tolerance, soldering process, test connectors, connecting cables and the surrounding test environment.

V. COMPARISON AND DISCUSSION

Comparison of the proposed MIMO antenna system with the recently published MIMO work operating in 13-14 GHz band is carried out in table 4. It summarizes several MIMO antenna parameters in terms of number of ports, size, bandwidth, mutual coupling, realized gain, radiation efficiency and

TABLE 4. Comparisons between the proposed MIMO antenna system and the published literature operating in 13-14 GHz band.

Ref.	Band (GHz)	N	Isolation enhancement technique	Gain (dBi)	Mutual coupling (dB)	Radiation efficiency %	ECC	DG (dB)	CCL (Bits/s/Hz)	ME (dB)	TARC (dB)	Size (mm^2)
[2] 2021	3-20	4	-	4	< -17	>75	< 0.01	> 9.97	NA	> -3	NA	38*38
[3] 2018	3.1-35	2	-	5	< -24	50-60	< 0.2	> 9.9	NA	NA	< -10	26*15
[7] 2019	13.24-13.88	2	-	8.52	< -20	63.3	0.0014	≈ 10	NA	NA	NA	26.3*22.6
[12] 2020	2.1-20	4	-	4	< -26	> 80	< 0.02	> 9.99	<0.4	NA	< -10	80*80
[26] 2018	Ku:13.8-14.6	2	Metasurface isolator	3.5-7.9	< -36	NA	NA	NA	NA	NA	NA	60*40
[28] 2020	7-16.5	2	DGS	NA	< -20	NA	<0.09	> 9.95	<0.23	NA	< -10	16*20
[29] 2018	7.8-16.5	4	Reduced ground plane and stubs	2	< -19	92	<0.14	9.9	NA	NA	< -4	25*25
[30] 2019	3.2-19.4	2	Inverted L-shaped stub	5.32	< -20	71-86	<0.1	> 9.95	NA	NA	< -30	18*30
[31] 2018	8.5-26.76	2	Dumbbell shaped slot	9	< -22	NA	< 0.002	> 9.95	NA	Na	NA	35*40
[39] 2020	2.9-40	4	Windmill-shaped structure	7	< -17	NA	< 0.04	> 9.5	<0.6	> -3	< -10	58*58
[40] 2018	10-16	3	Spacing: $\lambda/8$	6	< -25	50-60	< 0.006	≈ 10	NA	NA	NA	40*40
[41] 2019	3.5-19.44	2	Rectangular stub	4.95	< -20	71-89	< 0.05	> 9.95	NA	NA	< -20	20*45
[42] 2019	Ku:12-14.6	2	Metamaterial fractal load	6.5	< -40	80-82	NA	NA	NA	NA	NA	23*23
This work	**13.3-13.8**	**4**	**Three cascaded linear slots**	**8.8**	< -40 < -45	**86**	$< \mathbf{10}\times\mathbf{10}^{-5}$	$\approx \mathbf{10}$	$< \mathbf{0.3}$	> -1	< -10	**49*49**

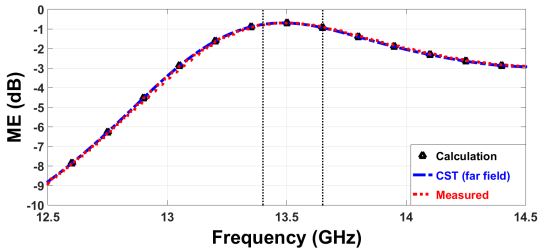

FIGURE 23. The ME performance of the proposed four-element MIMO antenna.

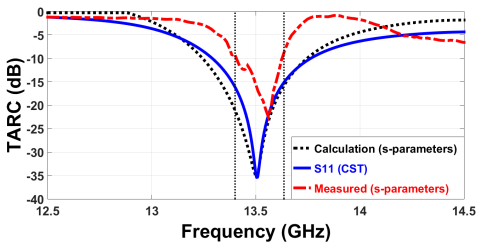

FIGURE 24. The TARC performance of the proposed four-element MIMO antenna.

different MIMO diversity performance parameters. Compared with [3], [7], [26], [28], [30], [31], [40]–[42], the proposed antenna has more ports. In terms of antenna size, the proposed antenna is more compact than [12], [39] which have same number of ports. Although antennas in [2], [29] are more compact, they achieve lower MIMO antenna performance in terms of realized gain, radiation efficiency and isolation between antenna elements. Generally, it is clear that the proposed designed MIMO antenna system performs well in terms of gain which reached 8.8 dBi, mutual coupling lower than -40 dB and good radiation efficiency of 86%. Although its size is not the smallest one, it shows significant high isolation improvement and better MIMO diversity performance compared to other literature work. This permits the proposed antenna to be utilized in real satellite communication applications. Furthermore, it is important to point out that the simplicity of proposed design and its symmetric geometry allow this design to be easily integrated to larger MIMO antennas with more radiation elements.

VI. CONCLUSION

A novel 4-element MIMO antenna system with high isolation fed by SIGW is presented. Designs using SIGW technology have the advantages of low dispersion and insertion loss. Thus, this design can be considered as a promising candidate for down-link satellite applications. The MIMO antenna element is of rectangular-shaped radiating slot to operate in band of 13.4-13.65 GHz. A prototype of the four-element MIMO antenna is fabricated. The measured and simulated results show good agreement in the entire operating band. Isolation enhancement technique of three linear cascaded slots between antenna elements is proposed to enhance isolation of lower than -40 dB. In addition, the

realized antenna gain is enhanced by 3-dBi. All the simulated and measured radiation results demonstrate that the proposed antenna offers important characteristics with stable high gain, acceptable radiation efficiency and good radiation patterns over the operating band. The diversity performance of proposed MIMO antenna structure is obtained by calculating different parameters like ECC, DG,,CCL, ME and TARC, which show a good diversity performance of the proposed antenna. A comparison with other reported antenna structures has been presented to highlight the novelty and significance of the proposed work. Therefore, the SIGW based highly isolated four-element MIMO antenna can be considered as an attractive candidate for real satellite applications.

REFERENCES

[1] R. Pokuls, J. Uher, and D. M. Pozar, "Microstrip antennas for SAR applications," *IEEE Trans. Antennas Propag.*, vol. 46, no. 9, pp. 1289–1296, Sep. 1998.

[2] W. Yin, S. Chen, J. Chang, C. Li, and S. K. Khamas, "CPW fed compact UWB 4-element MIMO antenna with high isolation," *Sensors*, vol. 21, no. 8, p. 2688, Apr. 2021.

[3] A. K. Gautam, S. Yadav, and K. Rambabu, "Design of ultra-compact UWB antenna with band-notched characteristics for MIMO applications," *IET Microw., Antennas Propag.*, vol. 12, no. 12, pp. 1895–1900, 2018.

[4] P.-D. Arapoglou, K. Liolis, M. Bertinelli, A. Panagopoulos, P. Cottis, and R. De Gaudenzi, "MIMO over satellite: A review," *IEEE Commun. Surveys Tuts.*, vol. 13, no. 1, pp. 27–51, 1st Quart. 2011.

[5] B. Ramamurthy, "MIMO for satellite communication systems," Ph.D. dissertation, Univ. South Australia, Adelaide, SA, Australia, Aug. 2018.

[6] R. T. Schwarz, A. Knopp, B. Lankl, D. Ogermann, and C. A. Hofmann, "Optimum-capacity MIMO satellite broadcast system: Conceptual design for LOS channels," in *Proc. 4th Adv. Satell. Mobile Syst.*, Aug. 2008, pp. 66–71.

[7] H. S. Gill, S. Singh, M. Singh, and G. Kaur, "Design of single-band MIMO antenna for Ku-band applications," in *Proc. Int. Conf. Electr., Electron. Comput. Eng. (UPCON)*, Nov. 2019, pp. 1–5.

[8] A. Perez-Neira, C. Ibars, J. Serra, A. del Coso, J. Gomez, and M. Caus, "MIMO applicability to satellite networks," in *Proc. 10th Int. Workshop Signal Process. Space Commun.*, Oct. 2008, pp. 1–9.

[9] S. Lu, H. T. Hui, and M. Bialkowski, "Optimizing MIMO channel capacities under the influence of antenna mutual coupling," *IEEE Antennas Wireless Propag. Lett.*, vol. 7, pp. 287–290, 2008.

[10] S.-W. Su, C.-T. Lee, and F.-S. Chang, "Printed MIMO-antenna system using neutralization-line technique for wireless USB-dongle applications," *IEEE Trans. Antennas Propag.*, vol. 60, no. 2, pp. 456–463, Feb. 2012.

[11] J. Zhu, S. Li, B. Feng, L. Deng, and S. Yin, "Compact dual-polarized UWB quasi-self-complementary MIMO/diversity antenna with band-rejection capability," *IEEE Antennas Wireless Propag. Lett.*, vol. 15, pp. 905–908, 2016.

[12] V. S. D. Rekha, P. Pardhasaradhi, B. T. P. Madhav, and Y. U. Devi, "Dual band notched orthogonal 4-element MIMO antenna with isolation for UWB applications," *IEEE Access*, vol. 8, pp. 145871–145880, 2020.

[13] J. Rahola and J. Ollikainen, "Analysis of isolation of two-port antenna systems using simultaneous matching," in *Proc. Eur. Conf. Antennas Propag. (EuCAP)*, Edinburgh, U.K., Nov. 2007, pp. 11–16.

[14] M. Ayatollahi, Q. Rao, and D. Wang, "A compact, high isolation and wide bandwidth antenna array for long term evolution wireless devices," *IEEE Trans. Antennas Propag.*, vol. 60, no. 10, pp. 4960–4963, Oct. 2012.

[15] W. Wu, B. Yuan, and A. Wu, "A quad-element UWB-MIMO antenna with band-notch and reduced mutual coupling based on EBG structures," *Int. J. Antennas Propag.*, vol. 2018, pp. 1–10, Feb. 2018.

[16] A. Ghalib and M. S. Sharawi, "TCM analysis of defected ground structures for MIMO antenna designs in mobile terminals," *IEEE Access*, vol. 5, pp. 19680–19692, 2017.

[17] M. Alibakhshikenari, F. Babaeian, B. S. Virdee, S. Aïssa, L. Azpilicueta, C. H. See, A. A. Althuwayb, I. Huynen, R. A. Abd-Alhameed, F. Falcone, and E. Limiti, "A comprehensive survey on 'various decoupling mechanisms with focus on metamaterial and metasurface principles applicable to SAR and MIMO antenna systems,"' *IEEE Access*, vol. 8, pp. 192965–193004, 2020.

[18] M. Alibakhshikenari, M. Khalily, B. S. Virdee, C. H. See, R. A. Abd-Alhameed, and E. Limiti, "Mutual-coupling isolation using embedded metamaterial EM bandgap decoupling slab for densely packed array antennas," *IEEE Access*, vol. 7, pp. 51827–51840, 2019.

[19] R. Anitha, P. V. Vinesh, K. C. Prakash, P. Mohanan, and K. Vasudevan, "A compact quad element slotted ground wideband antenna for MIMO applications," *IEEE Trans. Antennas Propag.*, vol. 64, no. 10, pp. 4550–4553, Oct. 2016.

[20] Z. Li, Z. Du, M. Takahashi, K. Saito, and K. Ito, "Reducing mutual coupling of MIMO antennas with parasitic elements for mobile terminals," *IEEE Trans. Antennas Propag.*, vol. 60, no. 2, pp. 473–481, Feb. 2012.

[21] S.-C. Chen, P.-W. Wu, C.-I.-G. Hsu, and J.-Y. Sze, "Integrated MIMO slot antenna on laptop computer for eight-band LTE/WWAN operation," *IEEE Trans. Antennas Propag.*, vol. 66, no. 1, pp. 105–114, Jan. 2018.

[22] M. Karaboikis, C. Soras, G. Tsachtsiris, and V. Makios, "Compact dual-printed inverted-F antenna diversity systems for portable wireless devices," *IEEE Antennas Wireless Propag. Lett.*, vol. 3, pp. 9–14, 2004.

[23] Z. Li, C. Yin, and X. Zhu, "Compact UWB MIMO Vivaldi antenna with dual band-notched characteristics," *IEEE Access*, vol. 7, pp. 38696–38701, 2019.

[24] A. Iqbal, O. A. Saraereh, A. W. Ahmad, and S. Bashir, "Mutual coupling reduction using F-shaped stubs in UWB-MIMO antenna," *IEEE Access*, vol. 6, pp. 2755–2759, 2018.

[25] R. Chandel, A. K. Gautam, and K. Rambabu, "Tapered fed compact UWB MIMO-diversity antenna with dual band-notched characteristics," *IEEE Trans. Antennas Propag.*, vol. 66, no. 4, pp. 1677–1684, Apr. 2018.

[26] M. Alibakhshikenari, B. S. Virdee, I. C. H. See, R. Abd-Alhameed, F. Falcone, A. Andújar, J. Anguera, and E. Limiti, "Study on antenna mutual coupling suppression using integrated metasurface isolator for SAR and MIMO applications," in *Proc. 48th Eur. Microw. Conf. (EuMC)*, 2018, pp. 1425–1428.

[27] M. Alibakhshikenari, B. S. Virdee, C. H. See, R. Abd-Alhameed, F. Falcone, and E. Limiti, "A new waveguide slot array antenna with high isolation and high antenna bandwidth operation on Ku- and K-bands for radar and MIMO systems," in *Proc. 15th Eur. Radar Conf. (EuRAD)*, Sep. 2018, pp. 401–404.

[28] A. K. Biswas and U. Chakraborty, "Textile multiple input multiple output antenna for X-band and Ku-band uplink-downlink applications," in *Proc. Nat. Conf. Emerg. Trends Sustain. Technol. Eng. Appl. (NCETSTEA)*, Feb. 2020, pp. 1–4.

[29] Nirdosh, C. M. Tan, and M. R. Tripathy, "A miniaturized T-shaped MIMO antenna for X-band and Ku-band applications with enhanced radiation efficiency," in *Proc. 27th Wireless Opt. Commun. Conf. (WOCC)*, Apr. 2018, pp. 1–5.

[30] N. Kumar, P. Kumar, and M. Sharma, "Superwideband dual notched band square monopole MIMO antenna for UWB/X/Ku band wireless applications," in *Proc. IEEE Indian Conf. Antennas Propogation (InCAP)*, Dec. 2019, pp. 1–5.

[31] Nirdosh, S. Sah, and A. Kakkar, "A two-element wideband MIMO antenna for X-band, Ku-band, K-band applications," in *Proc. 5th Int. Conf. Signal Process. Integr. Netw. (SPIN)*, Feb. 2018, pp. 94–97.

[32] L. Kong and X. Xu, "A compact dual-band dual-polarized microstrip antenna array for MIMO-SAR applications," *IEEE Trans. Antennas Propag.*, vol. 66, no. 5, pp. 2374–2381, May 2018.

[33] N. Bayat-Makou and A. A. Kishk, "Millimeter-wave substrate integrated dual level gap waveguide horn antenna," *IEEE Trans. Antennas Propag.*, vol. 65, no. 12, pp. 6847–6855, Dec. 2017.

[34] S. M. Sifat, M. M. M. Ali, S. I. Shams, and A.-R. Sebak, "High gain bow-tie slot antenna array loaded with grooves based on printed ridge gap waveguide technology," *IEEE Access*, vol. 7, pp. 36177–36185, 2019.

[35] S. I. Shams, M. A. Abdelaal, and A. A. Kishk, "Broadside uniform leaky-wave slot array fed by ridge gap splitted line," in *Proc. IEEE Int. Symp. Antennas Propag., USNC/URSI Nat. Radio Sci. Meeting*, Jul. 2015, pp. 2467–2468.

[36] C. Balanis, *Antenna Theory: Analysis and Design*, 2nd ed. New York, NY, USA: Wiley, 1997.

[37] A. A. Ibrahim and W. A. Ali, "High isolation 4-element ACS-fed MIMO antenna with band notched feature for UWB communications," *Int. J. Microw. Wireless Technol.*, vol. 14, no. 1, pp. 1–11, 2021.

[38] A. Abdelraheem, H. Elregaily, A. A. Mitkees, and M. Abdalla, "A hybrid isolation in two-element directive UWB MIMO antenna," *IETE J. Res.*, vol. 66, pp. 1–10, Oct. 2020.

[39] C. Yu, S. Yang, Y. Chen, W. Wang, L. Zhang, B. Li, and L. Wang, "A superwideband and high isolation MIMO antenna system using a windmill-shaped decoupling structure," *IEEE Access*, vol. 8, pp. 115767–115777, 2020.
[40] V. Satam and S. Nema, "High-gain overlapped elliptical shape diversity antenna for multiband applications," in *Proc. IEEE Indian Conf. Antennas Propogation (InCAP)*, Dec. 2018, pp. 1–5.
[41] M. Sharma, M. Kapil, and N. Kumar, "MIMO antenna with superwideband bandwidth including dual notched band characteristics for UWB/X/Ku band wireless applications," in *Proc. 3rd Int. Conf. Recent Develop. Control, Automat. Power Eng. (RDCAPE)*, Oct. 2019, pp. 185–190.
[42] M. Alibakhshikenari, M. Khalily, B. S. Virdee, C. H. See, R. Abd-Alhameed, and E. Limiti, "Mutual coupling suppression between two closely placed microstrip patches using EM-bandgap metamaterial fractal loading," *IEEE Access*, vol. 7, pp. 23606–23614, 2019.

M. S. H. SALAH EL-DIN was born in Egypt. He received the M.Sc. degree from the Arab Academy for Science and Technology (AASTMT), in 2016. He is currently pursuing the Ph.D. degree in electrical engineering with Ain Shams University, Egypt. His research interests include antenna design and MW technology.

SHOUKRY I. SHAMS (Member, IEEE) received the B.Sc. (Hons.) and M.Sc. degrees in electronics and communications engineering from Cairo University, Egypt, in 2004 and 2009, respectively, and the Ph.D. degree in electrical and computer engineering from Concordia University, Montreal, QC, Canada, in 2016. From 2005 to 2006, he worked as a Teaching and Research Assistant with the Department of Electronics and Communications Engineering, Cairo University. From 2006 to 2012, he worked as a Teaching and Research Assistant with the IET Department, German University in Cairo. From 2012 to 2016, he was a Teaching and Research Assistant with Concordia University, where he is currently an Affiliated Assistant Professor with the Department of Electrical and Computer Engineering. His research interests include microwave reciprocal/nonreciprocal design and analysis, high power microwave subsystems, antenna design, and material measurement. He received the Faculty Certificate of Honor, in 1999, the Distinction with Honor from Cairo University, in 2004, the Concordia University Recruitment Award, in 2012, and the Concordia University Accelerator.

A. M. M. A. ALLAM was born in Cairo, Egypt, in 1955. He received the B.S. degree in electrical engineering form MTC, in 1978, the M.S. degree in electrical engineering from Cairo University, in 1985, and the Ph.D. degree in electrical engineering from Kent University, U.K., in 1988. From 1978 to 1980, he was an Engineer in Airforce in Egyptian Army, working for maintenance and repair for airborne equipment in C-130 aircraft, where, he was a Crew Member in that interval. From 1981 to 1984, he was a Researcher and an Instructor with the air born equipment's Department, MTC, Cairo, where, he has been a Lecturer and a Researcher, since 1988. He granted Associate Professorship and Professorship, in 1995 and 2000, respectively. He was the Dean and the Deputy Commandant of the MTC. He was also the Dean and the Vice Dean of the Faculty of Information Engineering & Technology, German University in Cairo, Egypt, where he is currently the Head of the Communication Department. His research interests include RF and microwave technology, antenna design, smart antennas for vehicles and radar sensors, satellite communication, and diagnoses of censer based on the electromagnetic properties of human organisms. He did a lot of applied research in RADAR absorbing materials. He has published 100 conferences and journal papers.

ABDELHAMID GAAFAR received the B.Sc. degree in electrical engineering from the Military Technical College, Cairo, in 1977, the M.S. degree in electrical engineering from Al-Azhar University, Cairo, in 1983, and the Ph.D. degree in electrical engineering and applied science from George Washington University, Washington, DC, USA, in 1989. From 1980 to 1986, he was an Instructor with the EE Department, Military Technical College. From 1995 to 1998, he was the Head of the Electrical Engineering Department, Military Technical College. From 2002 to 2005, he was a Chief Assistant with the Technical Research Center, Egyptian Armed Forces. From 2005 to 2006, he was the Chief Assistant and the Head of the Research & Development Department Armament, Authority Egyptian Armed Forces. Since 2006, he has been a Professor in electrical engineering with the Electronic and Communication Department, Arab Academy for Science and Technology and Maritime Transport, Cairo Branch.

HADIA M. ELHENNAWY (Member, IEEE) received the B.Sc. and M.Sc. degrees from Ain Shams University, Cairo, Egypt, in 1972 and 1976, respectively, and the Doctorate of Engineering (Dr.-Ing.) degree from the Technische Universitat Braunschweig, Braunschweig, Germany, in 1982. Since 1992, she has been a Professor in communication engineering with the Electronics and Communications Engineering Department, Ain Shams University. In 2004, she became the Vice-Dean for graduate study and research. In 2005, she became the Dean of the Faculty of Engineering, Ain Shams University. Her research interests include microwave devices and subsystems, and filters and antennas for modern radar and wireless communications applications.

MOHAMED FATHY ABO SREE was born in Egypt. He received the M.Sc. degree from the Arab Academy for Science and Technology (AASTMT), in 2013, and the Ph.D. degree in electrical engineering from Ain Shams University, Egypt, in 2019. His research interests include antenna design and MW technology. He is reviewing in IEEE Access and *PIER* on-line journal.